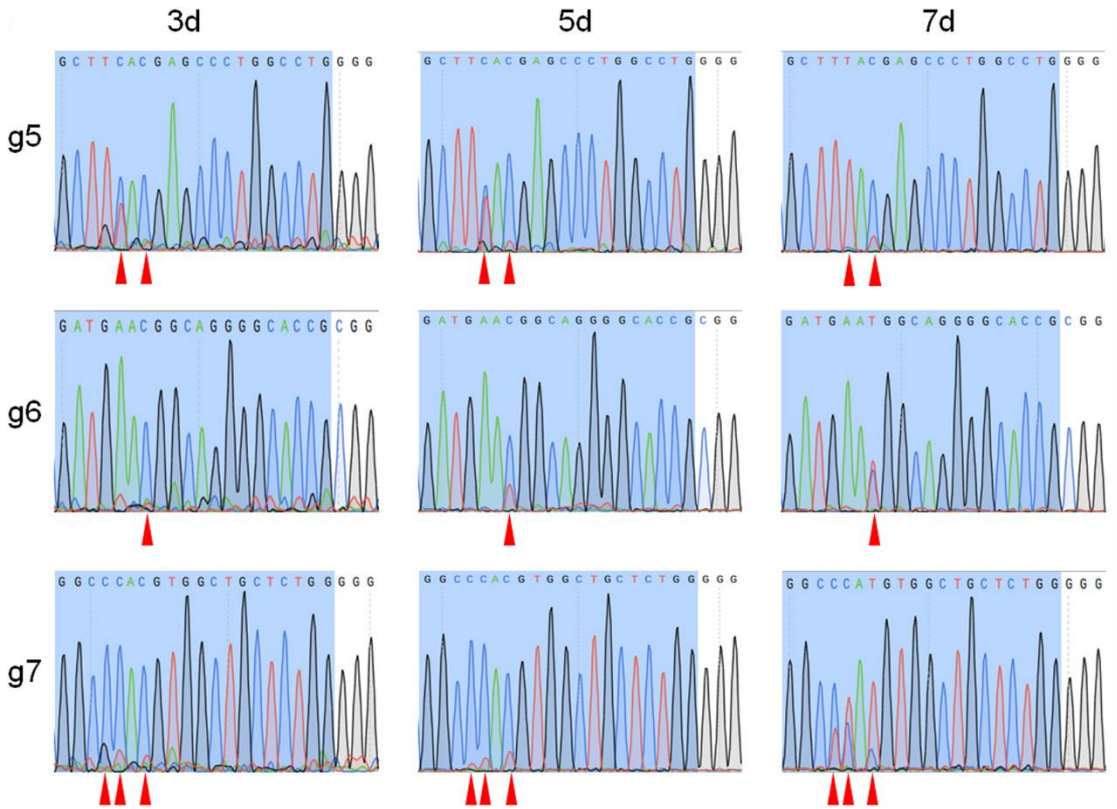

Supplementary Figure 1. Analysis of CBE base editing in different time points.

Conversion efficiencies at integrated sites (g5, g6 and g7) are measured at days 3, 5 and 7 after gRNA-target paired lentivirus infection. The red arrow indicates the base of the conversion.

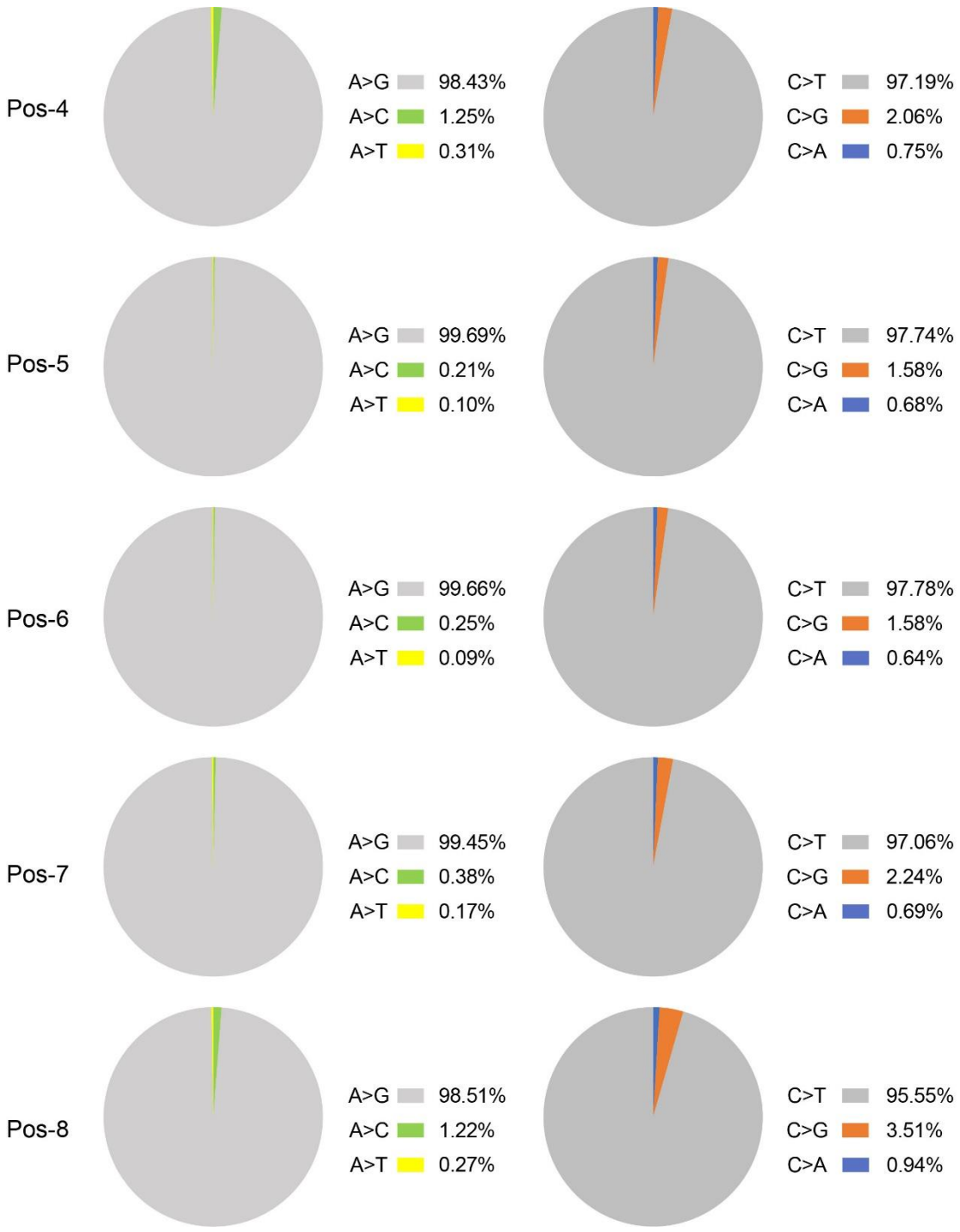

Supplementary Figure 2. The product purity of nucleotide conversion for ABE (left) and CBE (right).

The target nucleotide position is shown on the left.

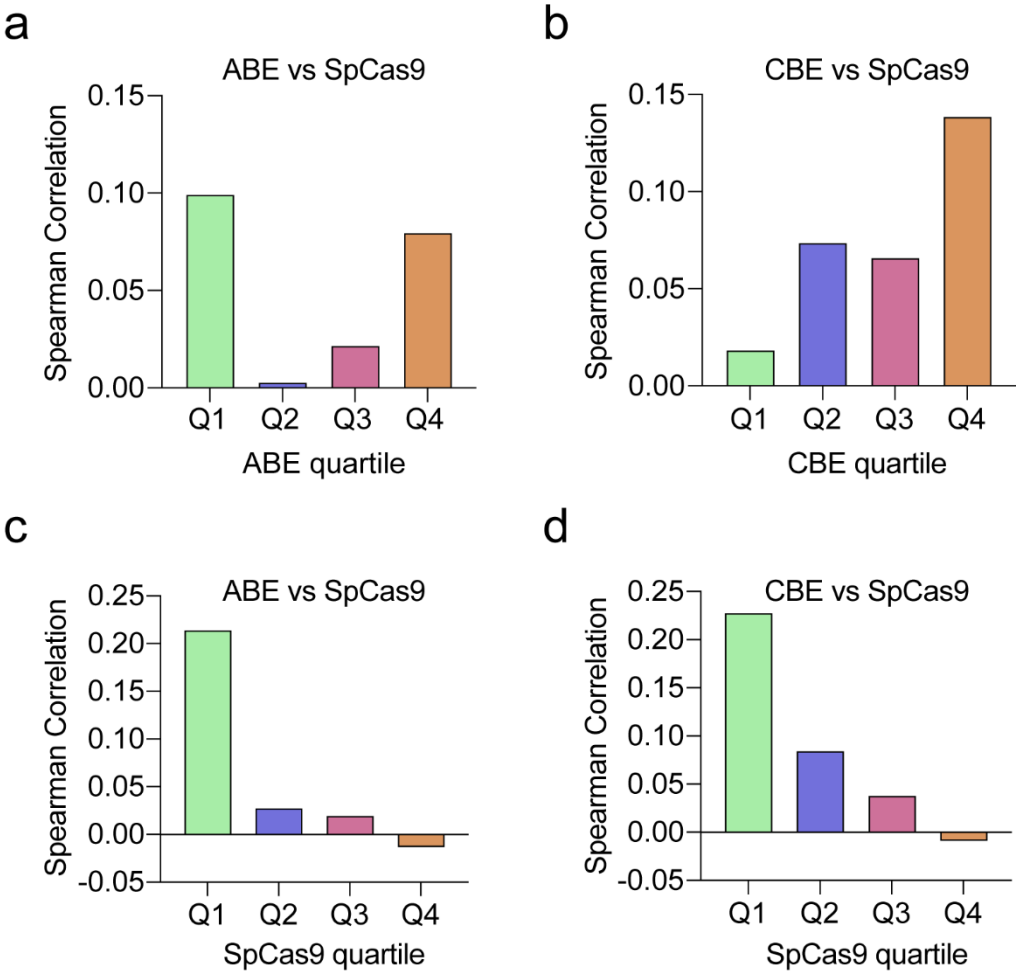

Supplementary Figure 3. Spearman correlation of editing efficiency between SpCas9 and base editors.

(**a**) Spearman correlation of editing efficiency between SpCas9 and ABE for each quartile of ABE editing efficiency. (**b**) Spearman correlation of editing efficiency between SpCas9 and CBE for each quartile of CBE editing efficiency. (**c**) Spearman correlation of editing efficiency between SpCas9 and ABE for each quartile of SpCas9 editing efficiency. (**d**) Spearman correlation of editing efficiency between SpCas9 and CBE for each quartile of SpCas9 editing efficiency.

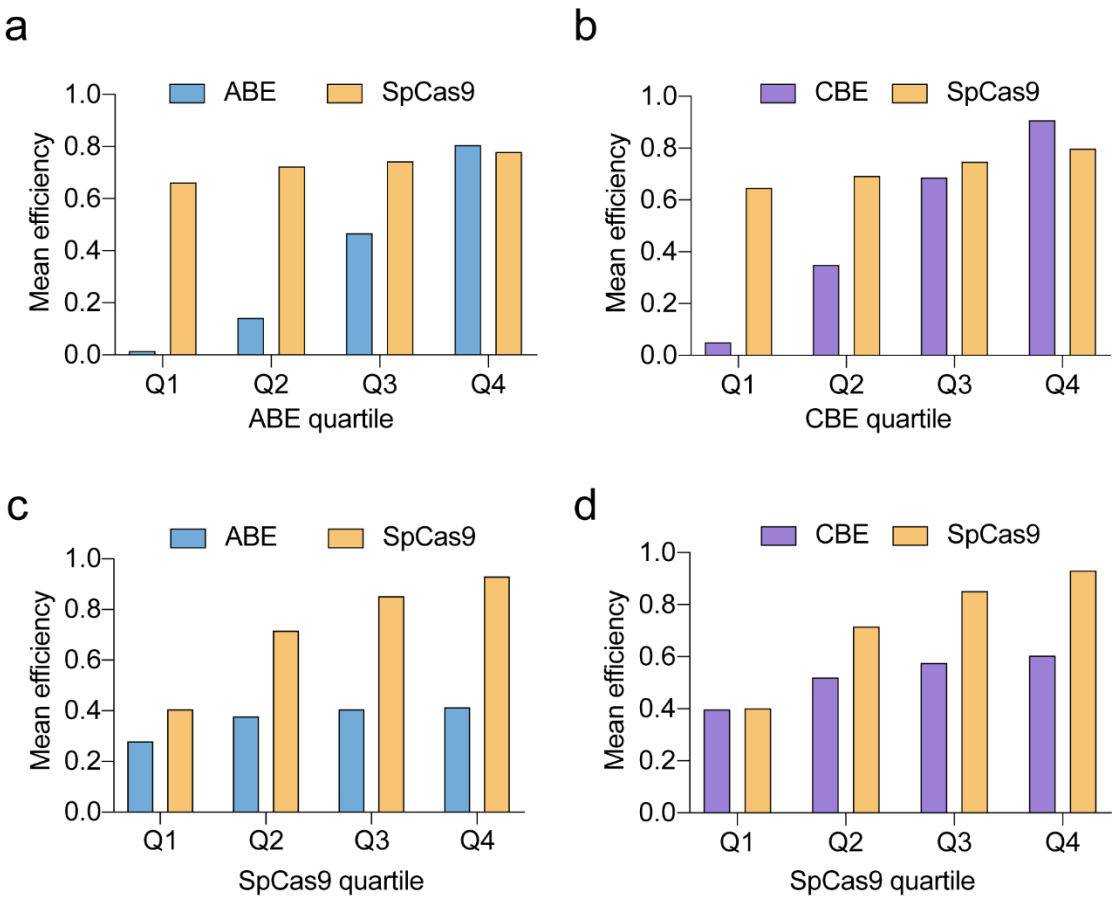

Supplementary Figure 4. Mean editing efficiency comparison between SpCas9 and base editors.

(**a**) Mean editing efficiency comparison between SpCas9 and ABE for each quartile of ABE editing efficiency. (**b**) Mean editing efficiency comparison between SpCas9 and CBE for each quartile of CBE editing efficiency. (**c**) Mean editing efficiency comparison between SpCas9 and ABE for each quartile of SpCas9 editing efficiency. (**d**) Mean editing efficiency comparison between SpCas9 and CBE for each quartile of SpCas9 editing efficiency.

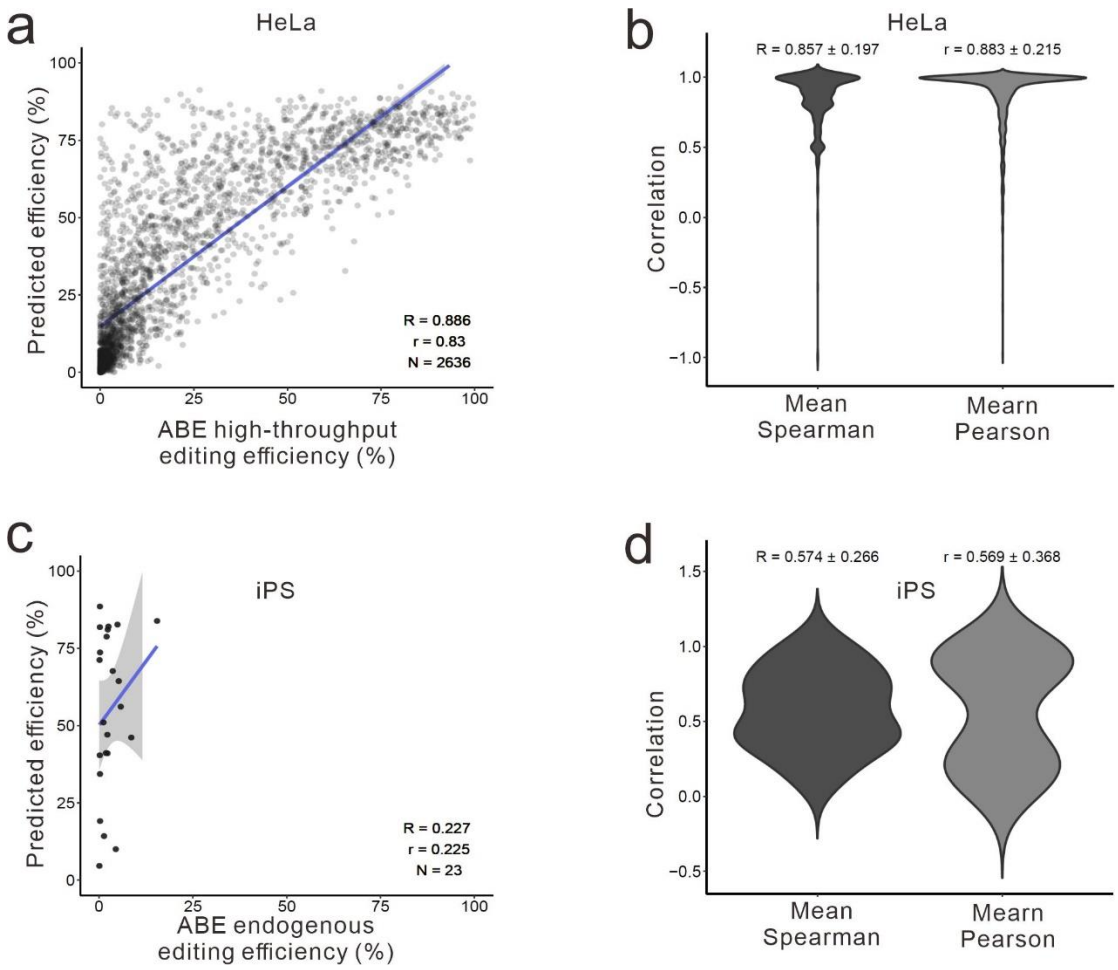

Supplementary Figure 5. Evaluation of ABEdeepon for conversion efficiency and outcome frequency prediction.

(**a**) Evaluation of ABEdeepon for conversion efficiency prediction at integrated targets in HeLa cells. (**b**) Evaluation of ABEdeepon for prediction of conversion outcome sequence frequencies at integrated targets in HeLa cells. (**c**) Evaluation of ABEdeepon for conversion efficiency prediction at endogenous targets in U2OS cells. (**c**) Evaluation of ABEdeepon for conversion efficiency prediction at endogenous targets in iPS cells. (**d**) Evaluation of ABEdeepon for prediction of conversion outcome sequence frequencies at endogenous targets in iPS cells.

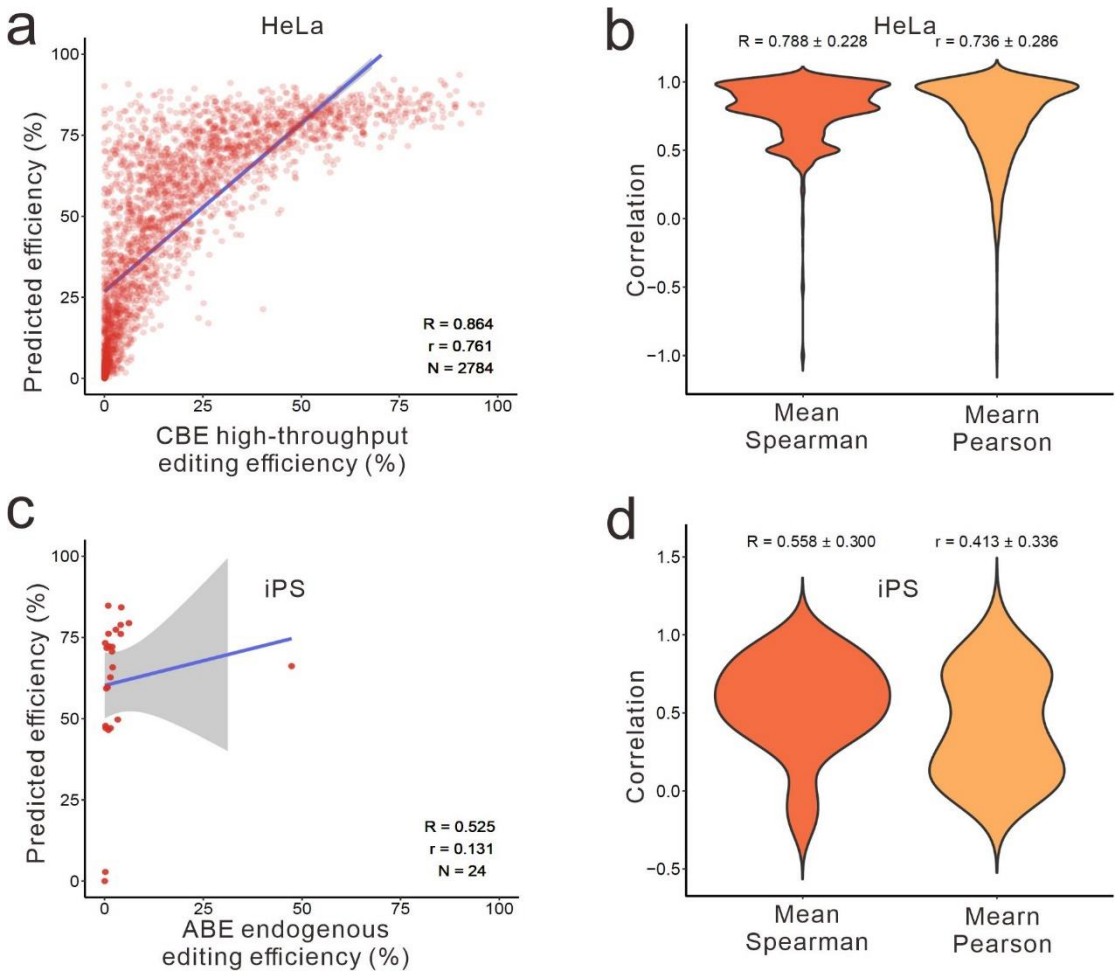

Supplementary Figure 6. Evaluation of CBEdeepon for conversion efficiency and outcome sequence prediction.

(**a**) Evaluation of CBEdeepon for conversion efficiency prediction at integrated targets in HeLa cells. (**b**) Evaluation of CBEdeepon for prediction of conversion outcome sequence frequencies at integrated targets in HeLa cells. (**c**) Evaluation of CBEdeepon for conversion efficiency prediction at endogenous targets in U2OS cells. (**c**) Evaluation of CBEdeepon for conversion efficiency prediction at endogenous targets in iPS cells. (**d**) Evaluation of CBEdeepon for prediction of conversion outcome sequence frequencies at endogenous targets in iPS cells.

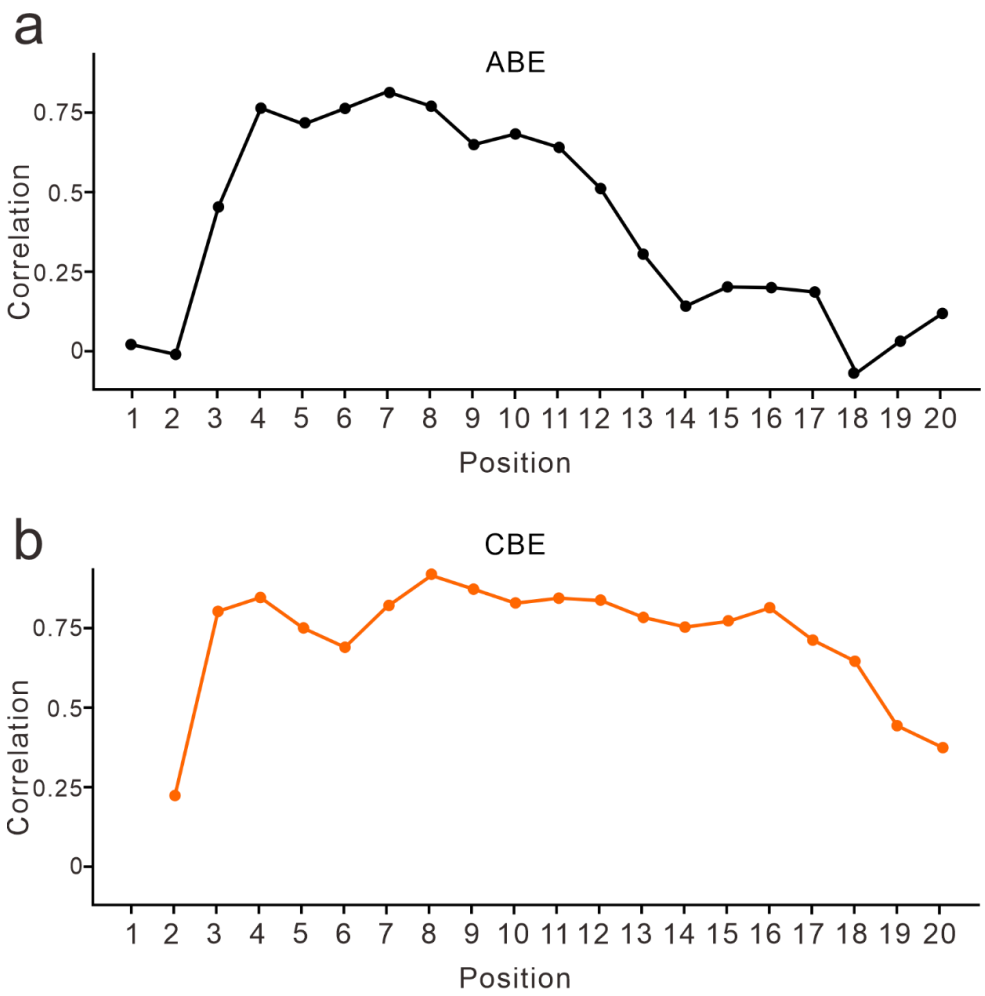

Supplementary Figure 7. Positional effects on prediction performance. (**a**) Spearman correlation of ABEdeepon at different position of targets. (**b**) Spearman correlation of CBEdeepon at different position of targets.